

# New Star-shaped Trinuclear Ru(II) Polypyridine Complexes of Imidazo[4,5-*f*][1,10]phenanthroline derivatives: Syntheses, Characterization, Photophysical and Electrochemical Properties

N. Arockia Samy and V. Alexander\*

Department of Chemistry, Loyola College, Chennai-600034, India.

## Electronic Supplementary Information (ESI)

**Figure S1.** 500 MHz  $^1\text{H}$  (a) and 125 MHz  $^{13}\text{C}$  (b) NMR spectrum of 2,4,6-trimethyl-1,3,5-tris(4-oxymethyl-1-formylphenyl)benzene (**2**) in  $\text{CDCl}_3$ .

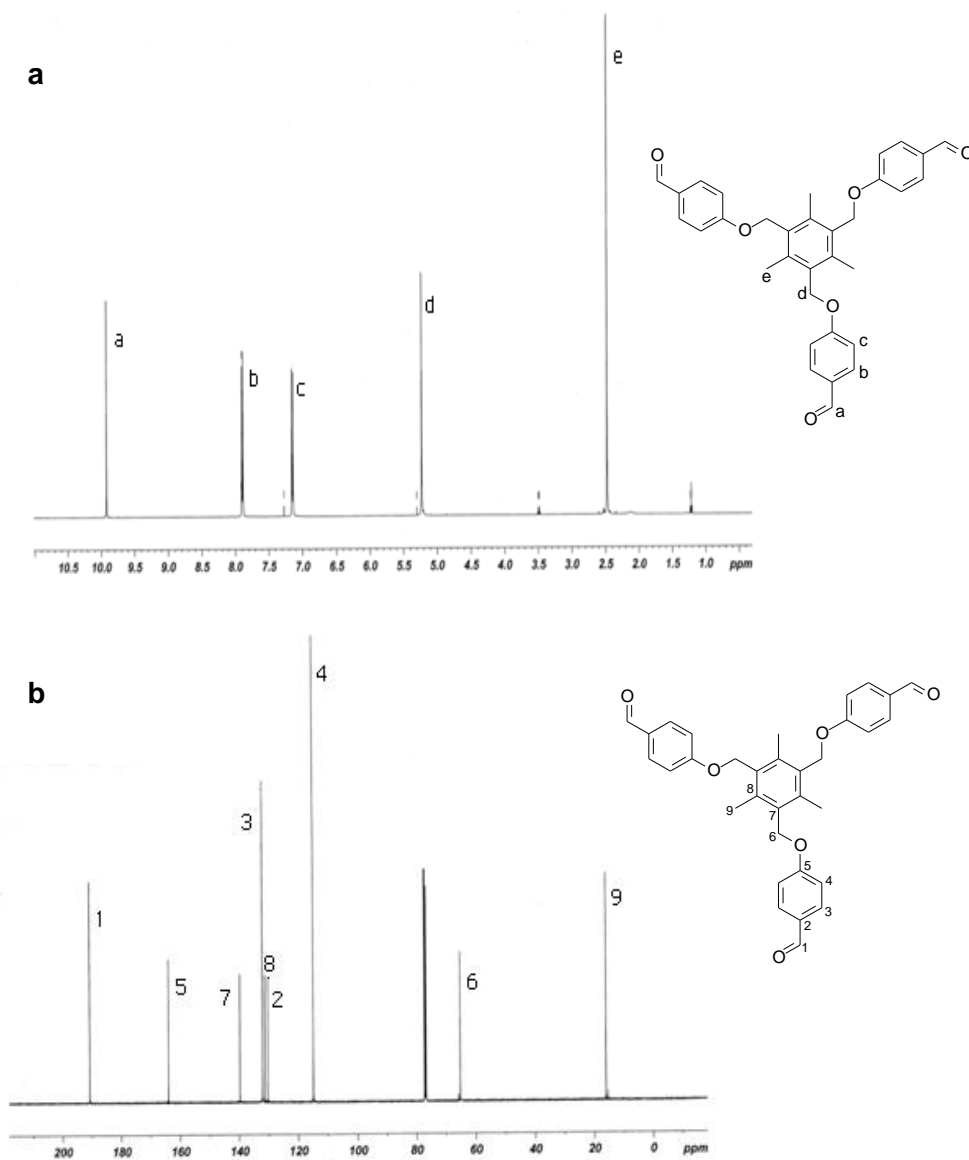


**Figure S2.** ESI mass spectrum of 2,4,6-trimethyl-1,3,5-tris(2-oxymethyl-1-formylphenyl)-benzene (**3**).

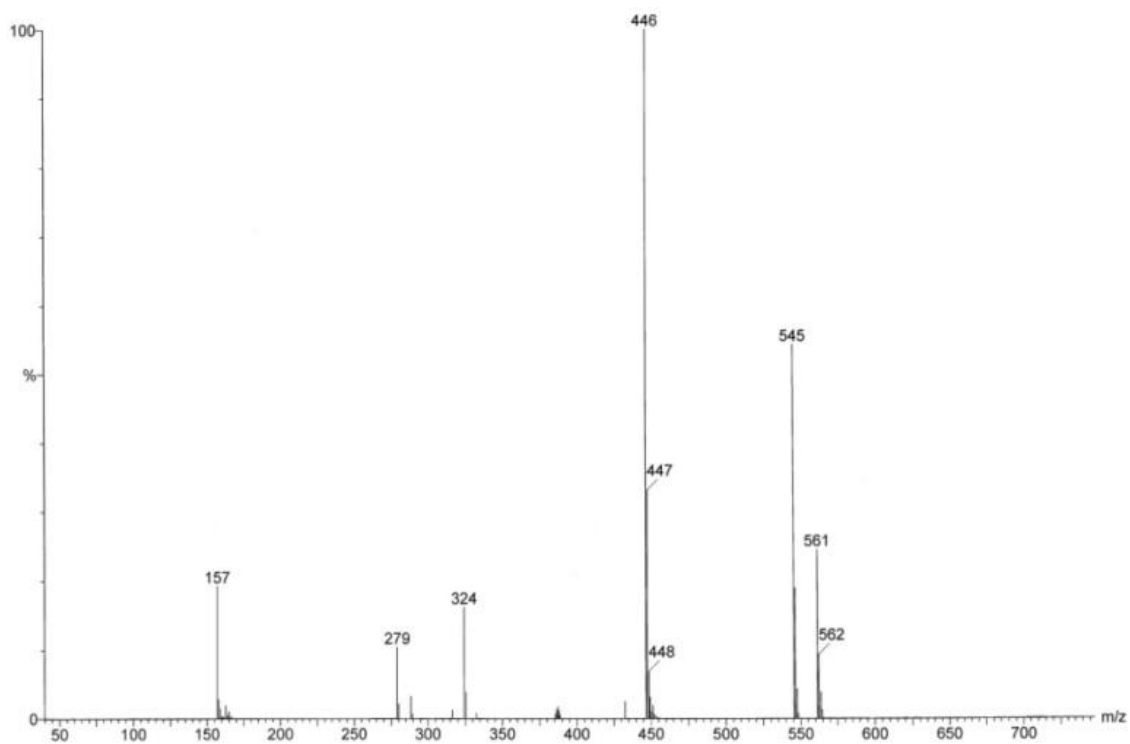


**Figure S3.** 500 MHz  $^1\text{H}$  (a) and 125 MHz  $^{13}\text{C}$  (b) NMR spectrum of 2,4,6-trimethyl-1,3,5-tris(2-oxymethyl-1-formylphenyl)benzene (**3**) in  $\text{CDCl}_3$ .

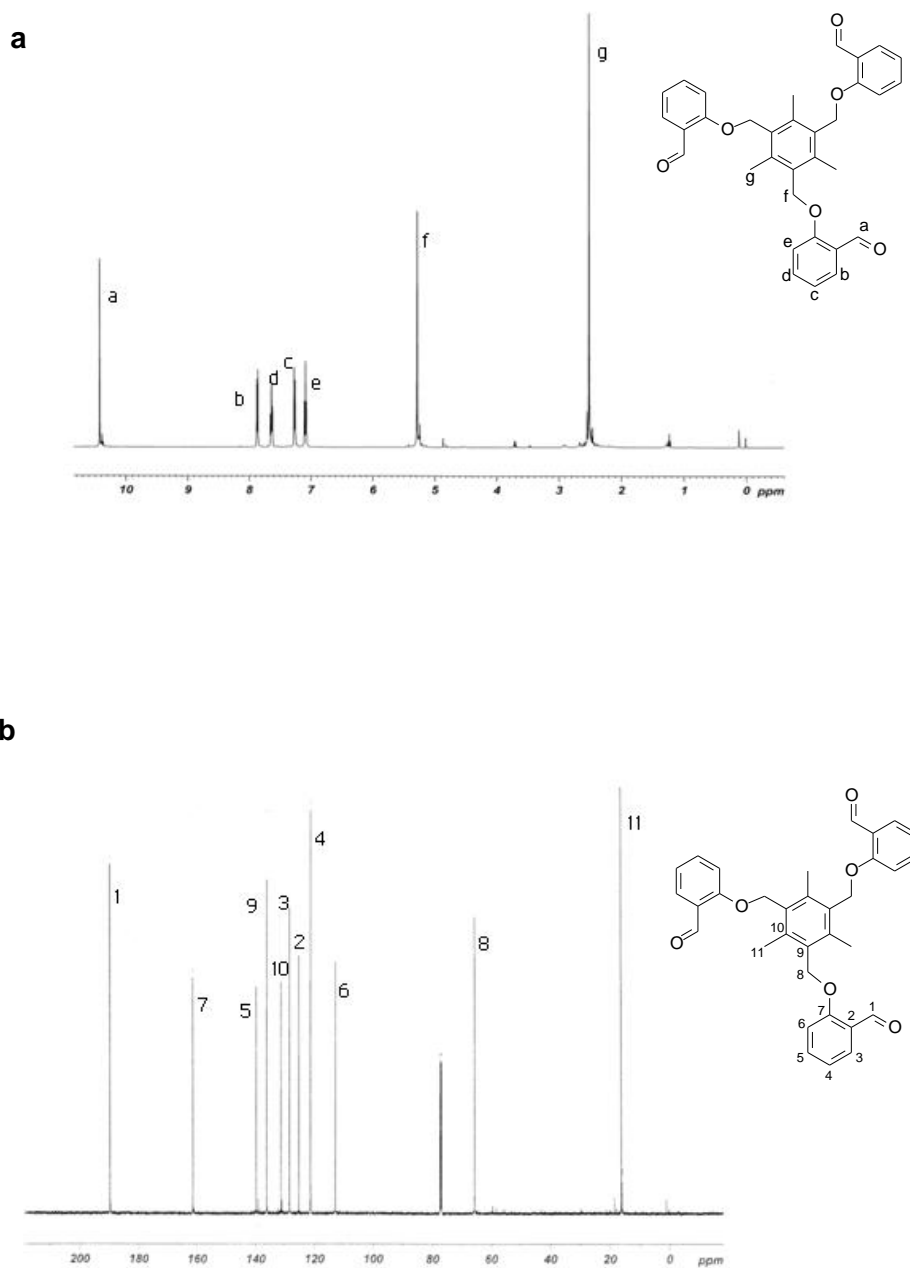


**Figure S4.** MALDI-TOF mass spectrum of 2,4,6-trimethyl-1,3,5-tris(4-oxymethyl-1-yl(1*H*-imidazo-2-yl[4,5-*f*][1,10]phenanthroline)phenyl)benzene (**4**).

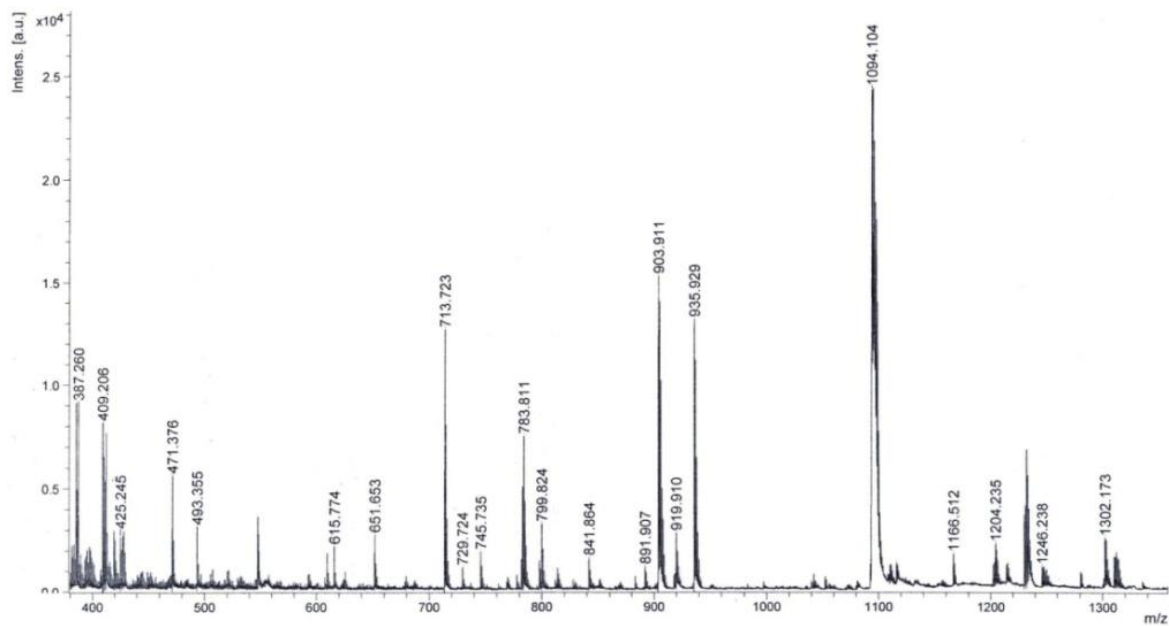


**Figure S5.** 500 MHz  $^1\text{H}$  (a) and 125 MHz  $^{13}\text{C}/\text{DEPT-135}$  (b) NMR spectrum of 2,4,6-trimethyl-1,3,5-tris(4-oxymethyl-1-yl(1*H*-imidazo-2-yl[4,5-*f*][1,10]-phenanthroline)phenyl)benzene (**4**) in  $\text{DMSO-}d_6$ .

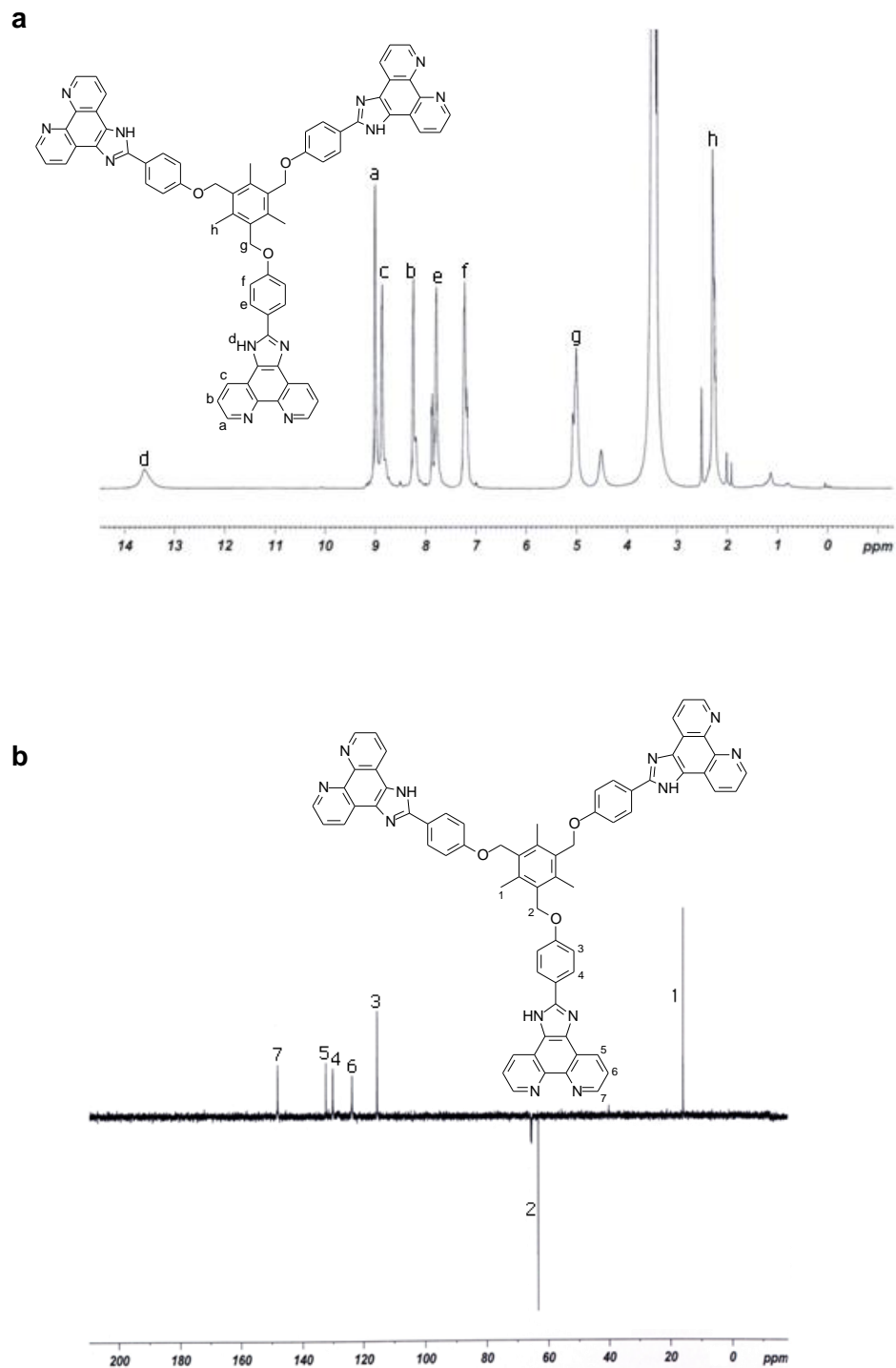


**Figure S6.** FAB mass spectrum of 2,4,6-trimethyl-1,3,5-tris(2-oxymethyl-1-yl(1*H*-imidazo-2-yl[4,5-*f*][1,10]phenanthroline)phenyl)benzene (**5**).

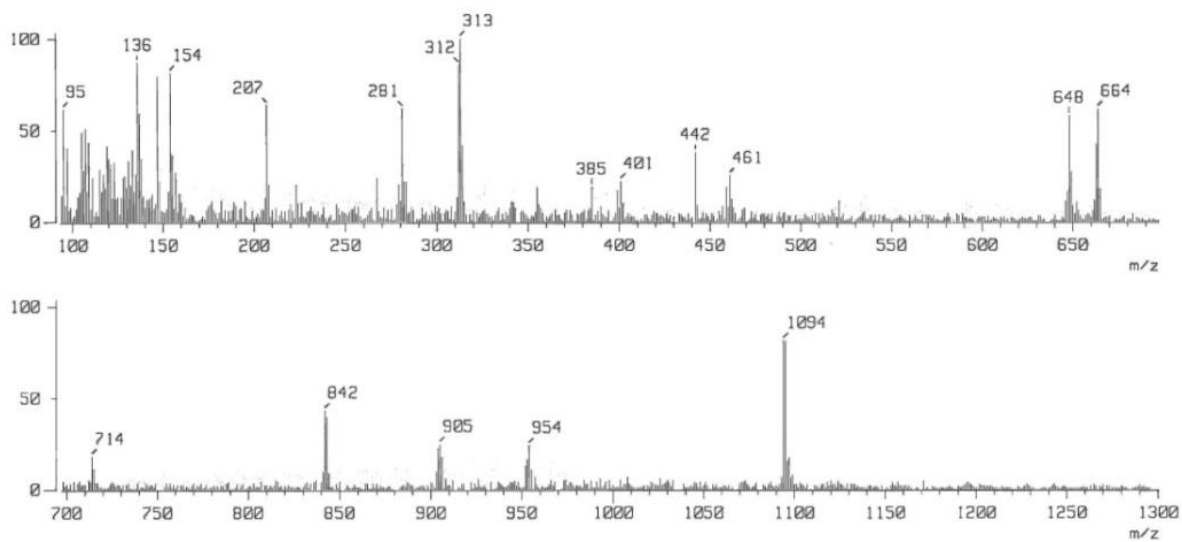


**Figure S7.** 500 MHz  $^1\text{H}$  (a) and 125 MHz  $^{13}\text{C}/\text{DEPT-135}$  (b) NMR spectrum of 2,4,6-trimethyl-1,3,5-tris(2-oxymethyl-1-yl(1*H*-imidazo-2-yl[4,5-*f*][1,10]-phenanthroline)phenyl)benzene (**5**) in  $\text{DMSO-}d_6$ .

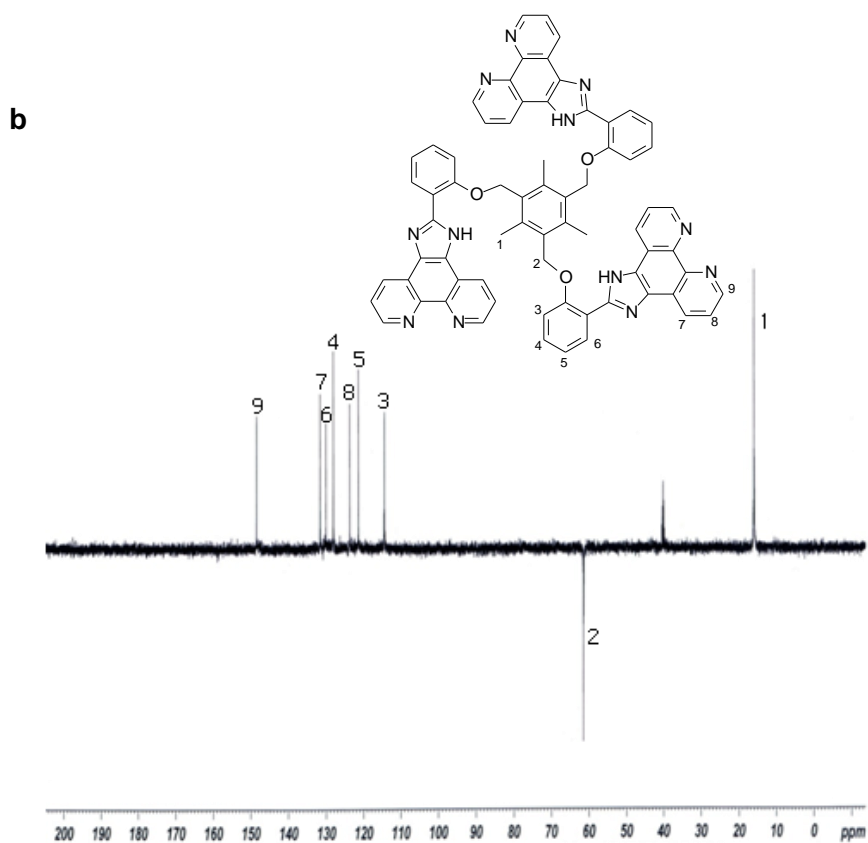
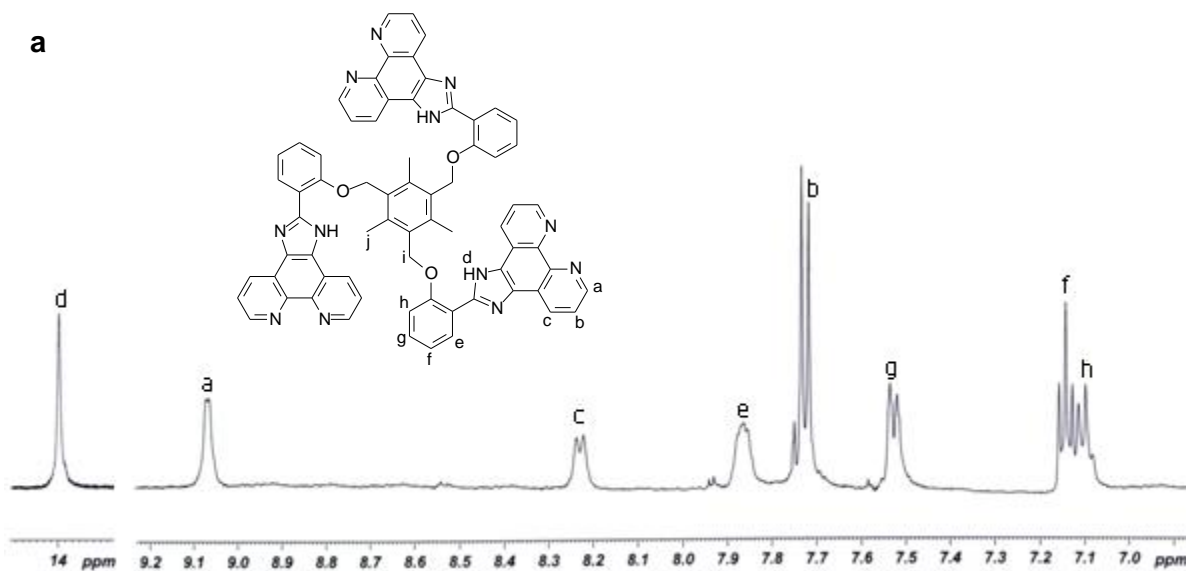


**Figure S8.** ESI mass spectrum of  $[\{\text{Ru}(\text{bpy})_2\}_3\{\mu\text{-mes}(1,4\text{-phO-Izphen})_3\}](\text{ClO}_4)_6 \cdot 4\text{H}_2\text{O}$  (6).

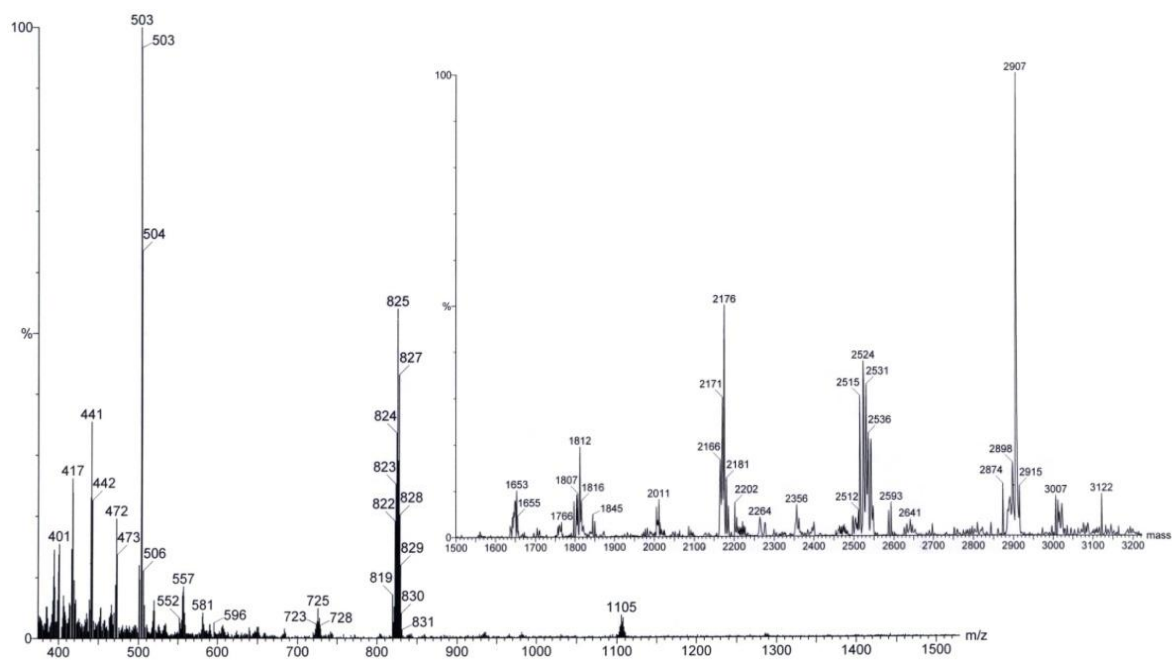


**Figure S9.** 125 MHz  $^{13}\text{C}/\text{DEPT-135}$  NMR spectrum of  $[\{\text{Ru}(\text{bpy})_2\}_3\{\mu\text{-mes}(1,4\text{-phO-Izphen})_3\}](\text{ClO}_4)_6 \cdot 4\text{H}_2\text{O}$  (**6**) in  $\text{DMSO-}d_6$ .

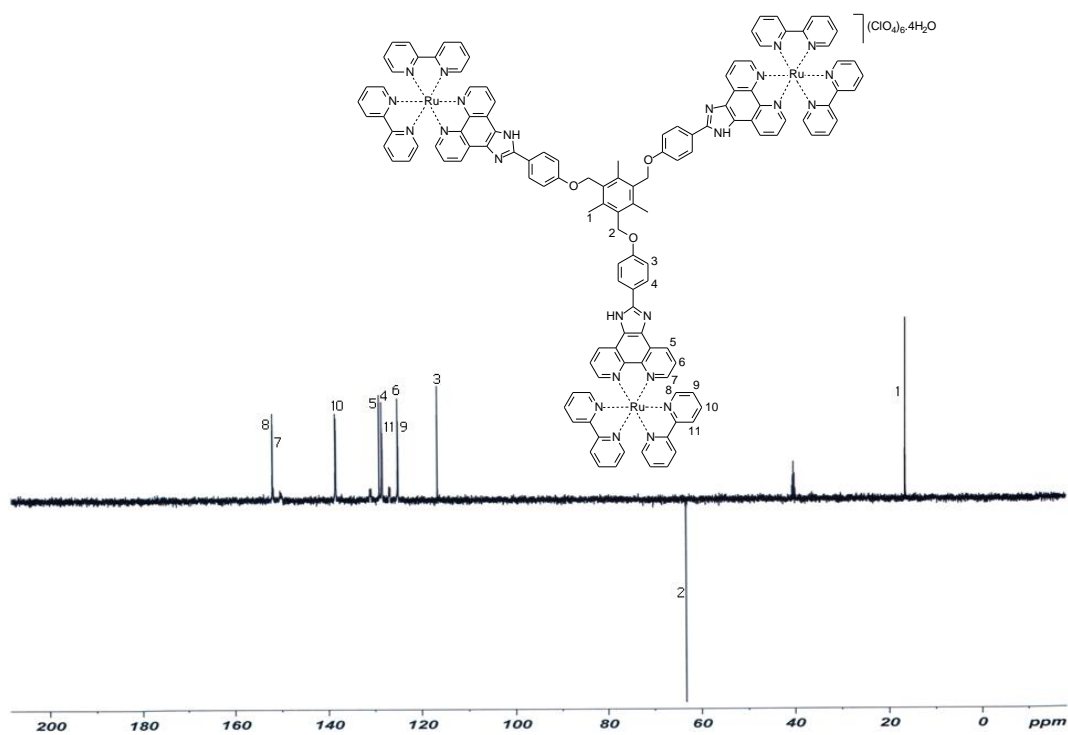


**Figure S10.** Cyclic voltammogram of  $[\{\text{Ru}(\text{bpy})_2\}_3\{\mu\text{-mes}(1,4\text{-phO-Izphen})_3\}](\text{ClO}_4)_6 \cdot 4\text{H}_2\text{O}$  (**6**) on a glassy carbon millielectrode in acetonitrile (0.1 M  $\text{Et}_4\text{NClO}_4$ ) versus  $\text{Ag}/\text{AgCl}$  at 25 °C, scan rate = 50  $\text{mV s}^{-1}$ .

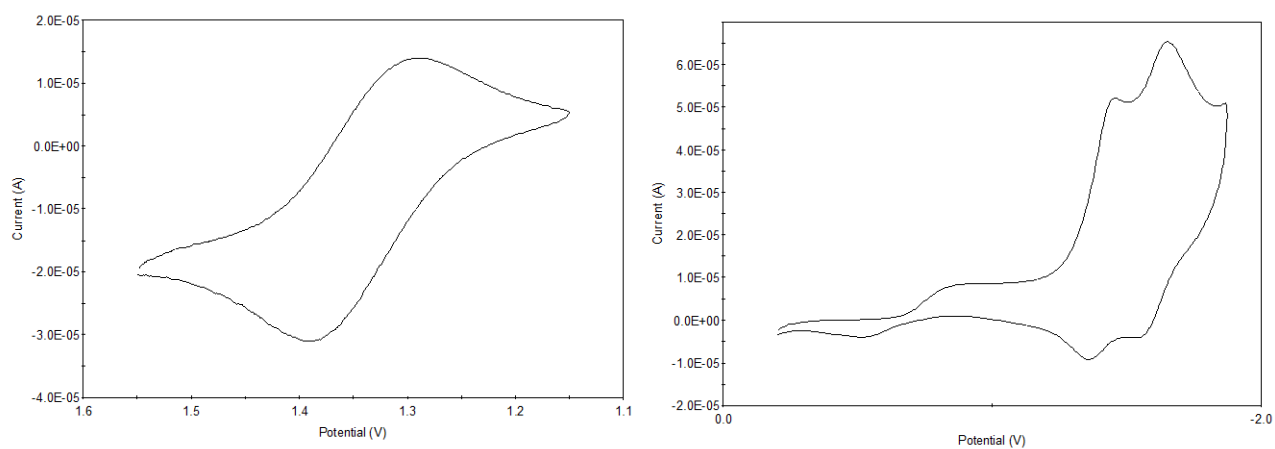


**Figure S11.** ESI mass spectrum of  $[\{\text{Ru}(\text{phen})_2\}_3\{\mu\text{-mes}(1,4\text{-phO-Izphen})_3\}](\text{ClO}_4)_6 \cdot 3\text{H}_2\text{O}$  (**7**).

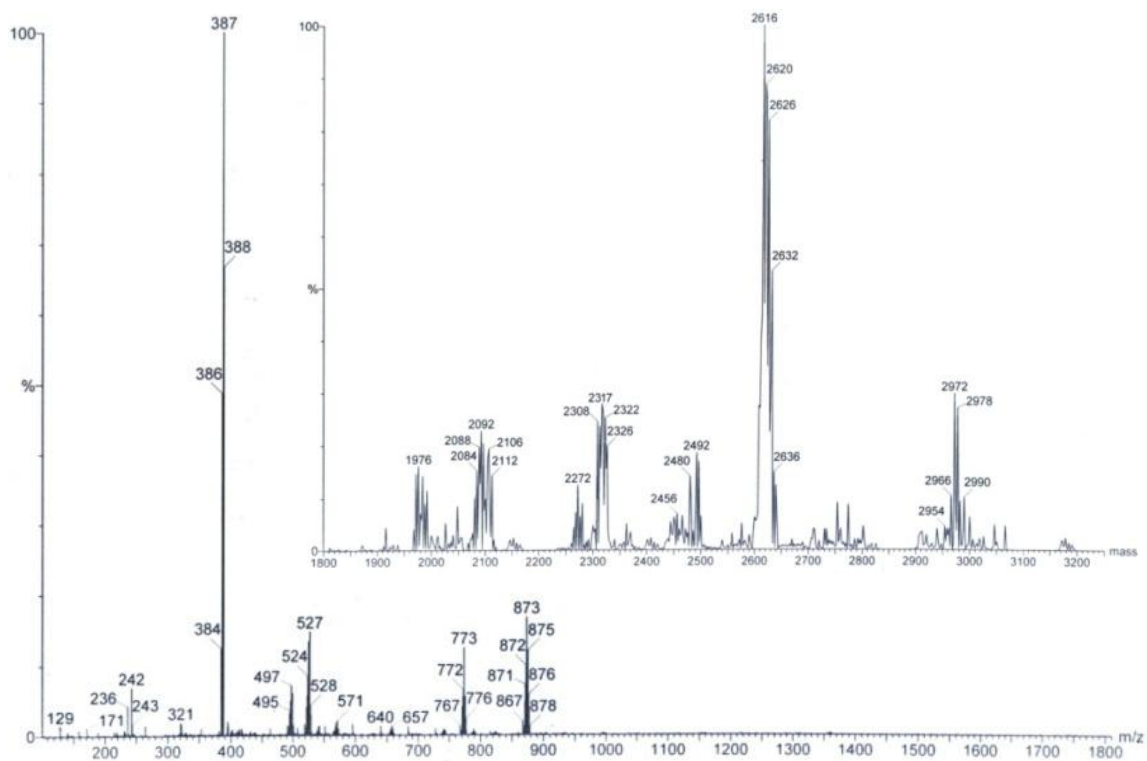


**Figure S12.** 125 MHz  $^{13}\text{C}/\text{DEPT-135}$  NMR spectrum of  $[\{\text{Ru}(\text{phen})_2\}_3\{\mu\text{-mes}(1,4\text{-phO-Izphen})_3\}](\text{ClO}_4)_6 \cdot 3\text{H}_2\text{O}$  (**7**) in  $\text{DMSO-}d_6$ .

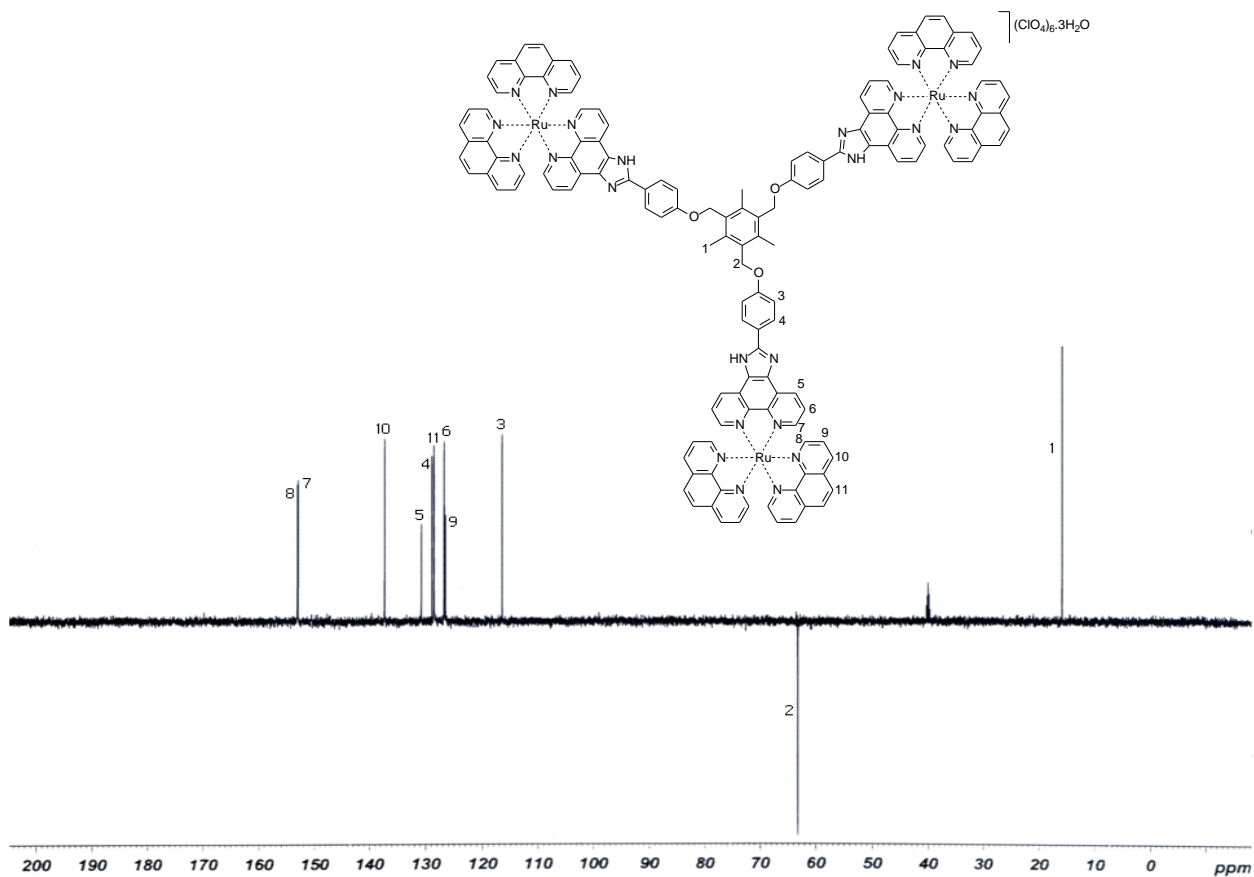


**Figure S13.** Cyclic voltammogram of  $[\{\text{Ru}(\text{phen})_2\}_3\{\mu\text{-mes}(1,4\text{-phO-Izphen})_3\}](\text{ClO}_4)_6 \cdot 3\text{H}_2\text{O}$  (**7**) on a glassy carbon millielectrode in acetonitrile (0.1 M  $\text{Et}_4\text{NClO}_4$ ) versus Ag/AgCl at 25 °C, scan rate = 50  $\text{mV s}^{-1}$ .

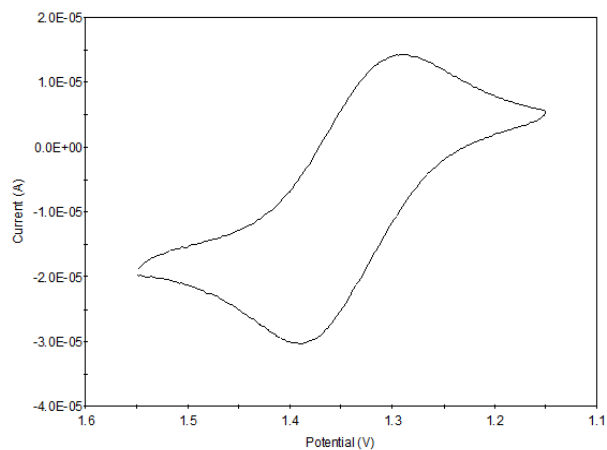


**Figure S14.** ESI mass spectrum of  $[\{\text{Ru}(\text{bpy})_2\}_3\{\mu\text{-mes}(1,2\text{-phO-Izphen})_3\}](\text{ClO}_4)_6 \cdot 4\text{H}_2\text{O}$  (**8**).

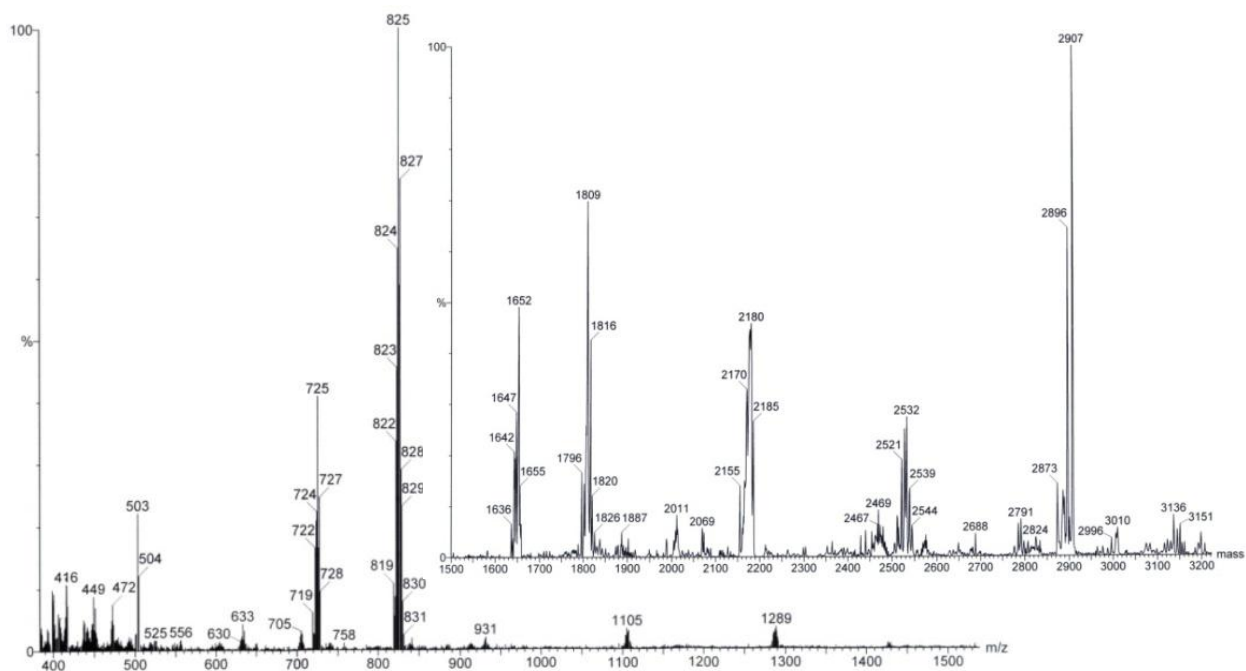


**Figure S15.** 125 MHz  $^{13}\text{C}$  NMR spectrum of  $[\{\text{Ru}(\text{bpy})_2\}_3\{\mu\text{-mes}(1,2\text{-phO-Izphen})_3\}](\text{ClO}_4)_6 \cdot 4\text{H}_2\text{O}$  (**8**) in  $\text{DMSO-}d_6$ .

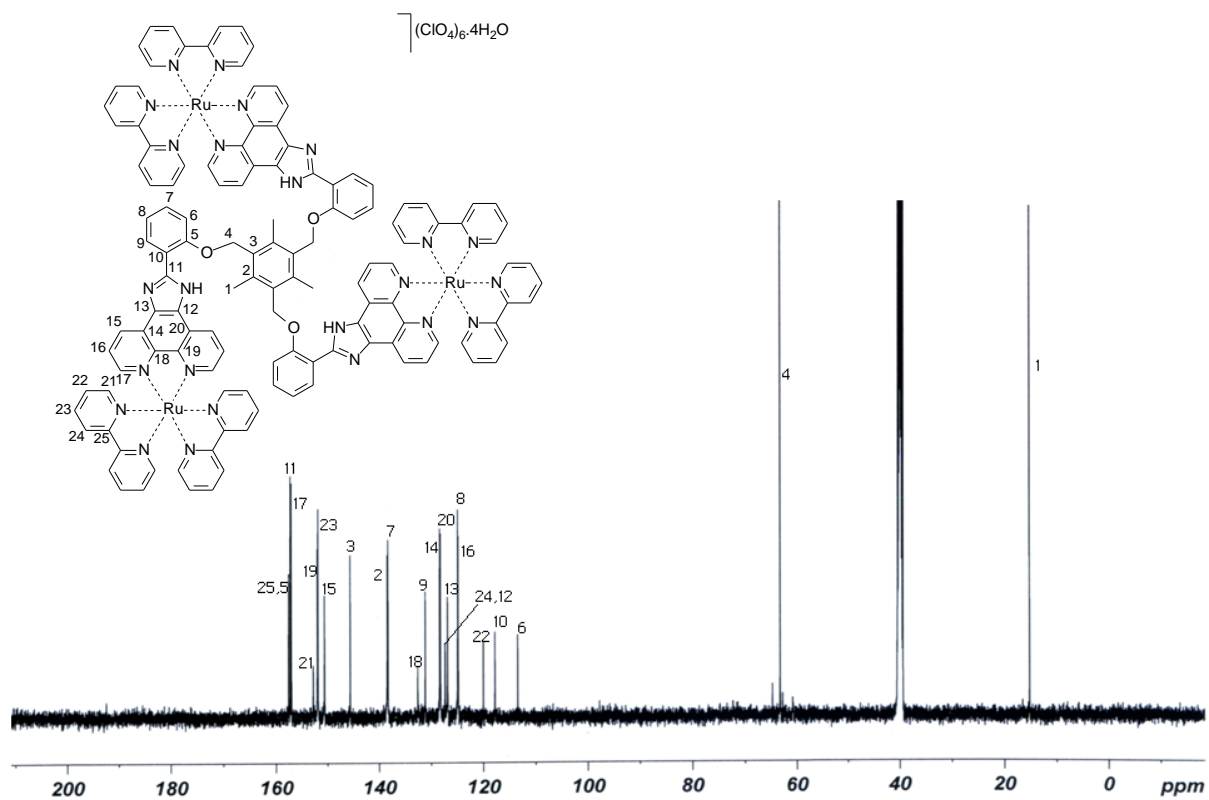


**Figure S16.** Cyclic voltammogram of  $[\{\text{Ru}(\text{bpy})_2\}_3\{\mu\text{-mes}(1,2\text{-phO-Izphen})_3\}](\text{ClO}_4)_6 \cdot 4\text{H}_2\text{O}$  (**8**) on a glassy carbon millielectrode in acetonitrile (0.1 M  $\text{Et}_4\text{NClO}_4$ ) versus Ag/AgCl at 25 °C, scan rate = 50  $\text{mV s}^{-1}$ .

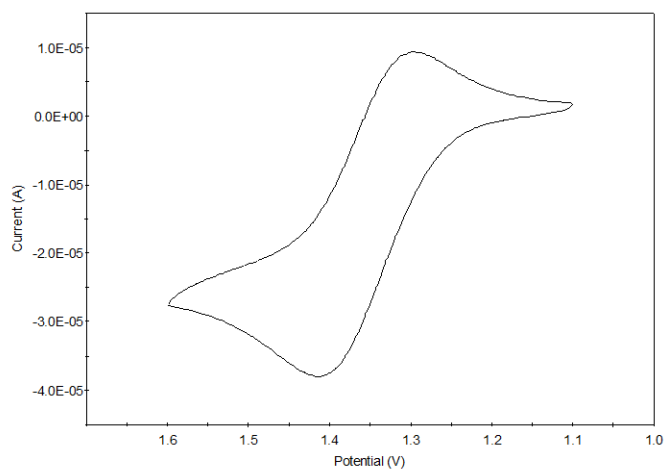


**Figure S17.** ESI mass spectrum of  $[\{\text{Ru}(\text{phen})_2\}_3\{\mu\text{-mes}(1,2\text{-phO-Izphen})_3\}](\text{ClO}_4)_6 \cdot 3\text{H}_2\text{O}$  (**9**).

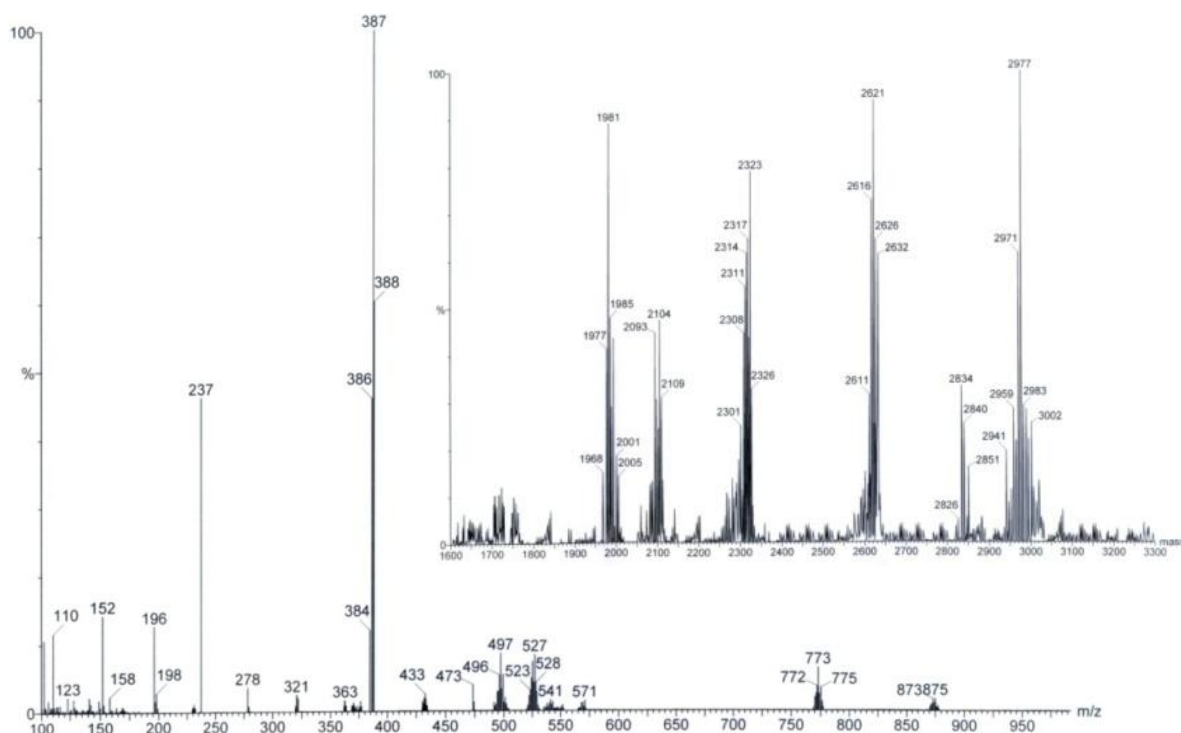


**Figure S18.** 125 MHz  $^{13}\text{C}/\text{DEPT}-135$  NMR spectrum of  $[\{\text{Ru}(\text{phen})_2\}_3\{\mu\text{-mes}(1,2\text{-phO-Izphen})_3\}](\text{ClO}_4)_6 \cdot 3\text{H}_2\text{O}$  (**9**) in  $\text{DMSO}-d_6$ .

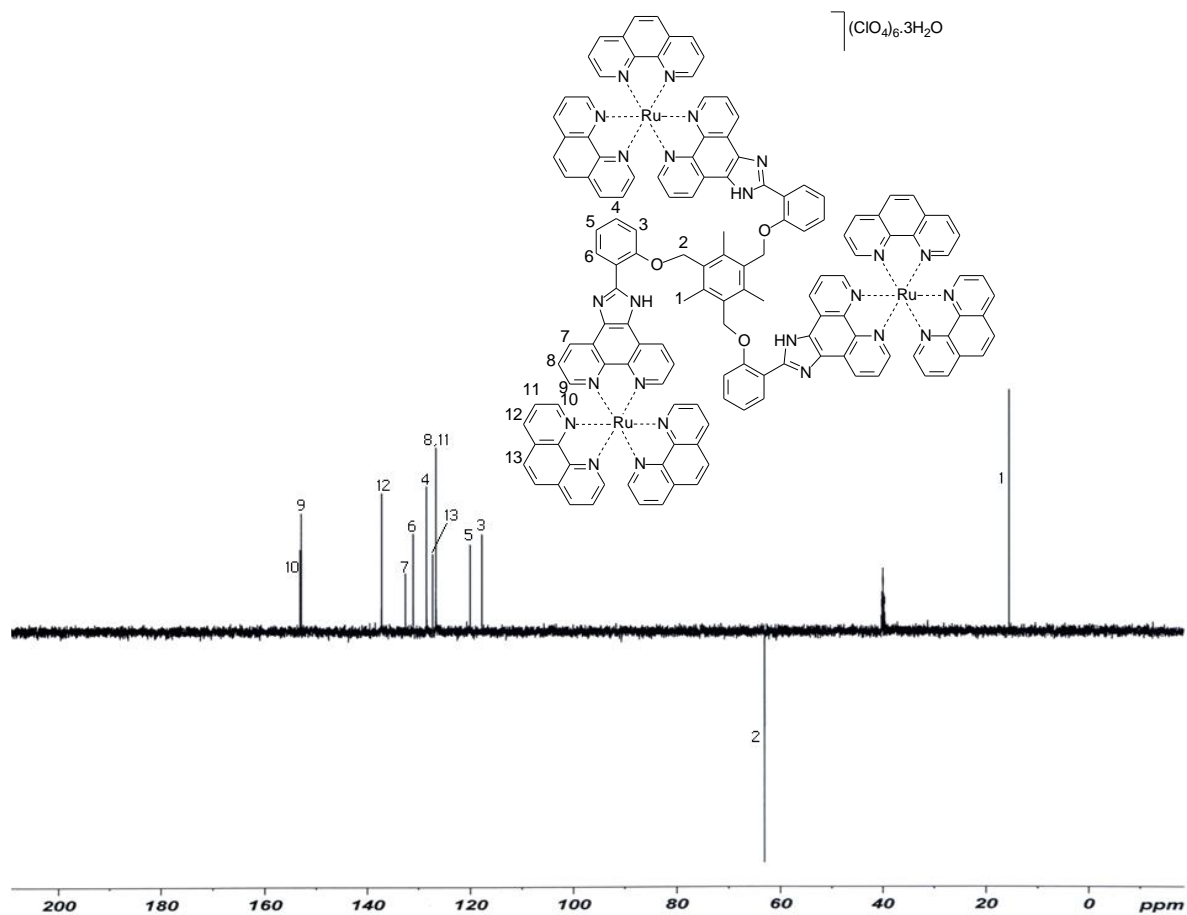


**Figure S19.** Cyclic voltammogram of  $[\{\text{Ru}(\text{phen})_2\}_3\{\mu\text{-mes}(1,2\text{-phO-Izphen})_3\}](\text{ClO}_4)_6 \cdot 3\text{H}_2\text{O}$  (**9**) on a glassy carbon millielectrode in acetonitrile (0.1 M  $\text{Et}_4\text{NClO}_4$ ) versus Ag/AgCl at 25 °C, scan rate = 50 mV s<sup>-1</sup>.

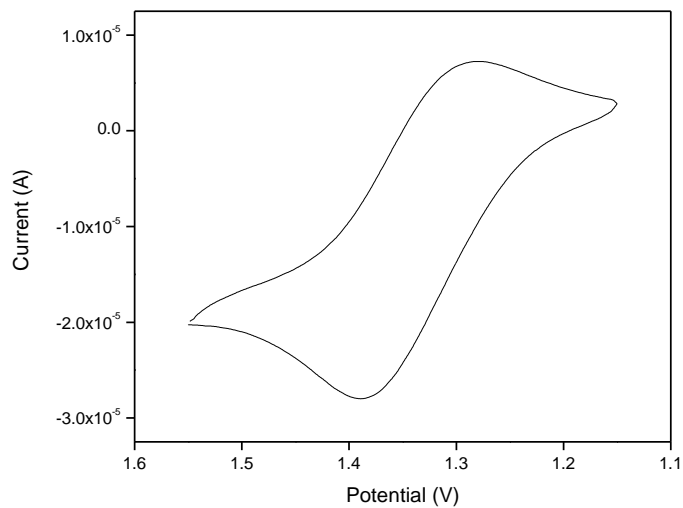


**Figure S20.** Electronic absorption spectrum (a) and emission spectrum (b) of mes(1,4-phO-Izphen)<sub>3</sub> (4) in DMF at room temperature. inset: excitation spectrum of 4.

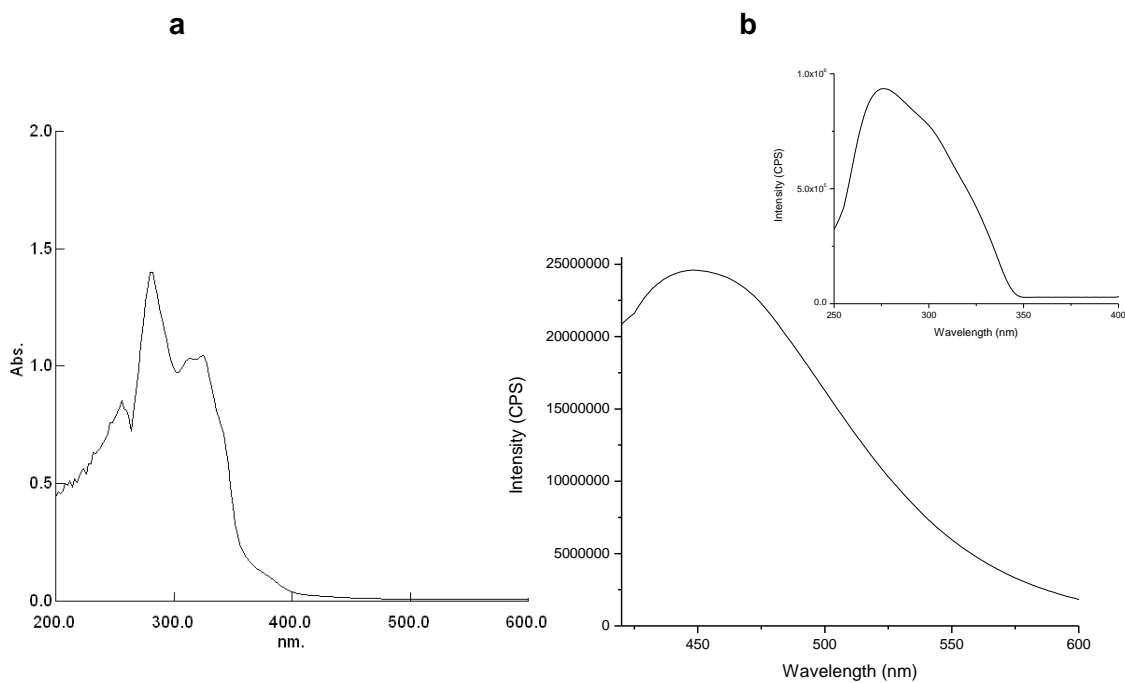


**Figure S21.** Electronic absorption spectrum (a) and emission spectrum (b) of mes(1,2-phO-Izphen)<sub>3</sub> (**5**) in DMF at room temperature. inset: excitation spectrum of **5**.

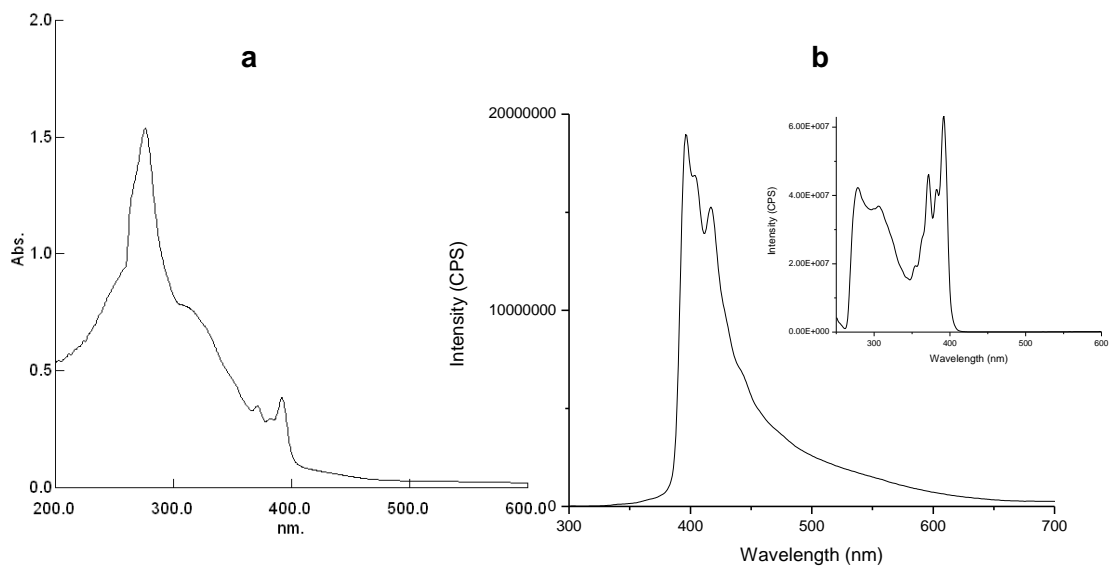


**Figure S22.** Cyclic voltammogram of  $[\{\text{Ru}(\text{bpy})_2\}_3\{\mu\text{-mes}(1,2\text{-phO-Izphen})_3\}](\text{ClO}_4)_6 \cdot 4\text{H}_2\text{O}$  (**8**) in the potential range +2 to -2 V on a glassy carbon millielectrode in acetonitrile (0.1 M  $\text{Et}_4\text{NClO}_4$ ) versus Ag/AgCl at 25 °C, scan rate = 50  $\text{mV s}^{-1}$ .

